Deletion of Clock Gene *Period1* (*Per1*) in Neurons but not in Astrocytes Shortens Clock Period and diminishes Light-Mediated Rapid Phase Advances in Mice

Dan-Adrian Epuran and Urs Albrecht *

Posted Date: 16 October 2025

doi: 10.20944/preprints202510.1246.v1

Keywords: light; resetting; phase shift; entrainment; advance; delay; *Per1* knockout

 doi:10.20944/preprints202510.1246.v1

Article

Deletion of Clock Gene *Period1* (*Per1*) in Neurons but not in Astrocytes Shortens Clock Period and diminishes Light-Mediated Rapid Phase Advances in Mice

Dan-Adrian Epuran [1] and Urs Albrecht

Dept. Of Biology, University of Fribourg, 1700 Fribourg, Switzerland; urs.albrecht@unifr.ch

Abstract

The circadian clock enables organisms to anticipate daily recurring events and synchronize their internal rhythms with environmental cues, such as light, aligning with the day/night cycle. Central to the molecular mechanisms of the circadian clock and light sensing are the *Period* (*Per*) 1 and 2 genes. While the roles of *Per2* in astrocytes and neurons have been characterized, the specific contributions of *Per1* remain less understood. Previous research has shown that *Per2* in neurons, but not astrocytes, influences phase shifts, whereas the regulation of circadian period involves *Per2* in both cell types. In this study, we investigated the role of *Per1* in neurons and astrocytes in modulating circadian period and phase shifts. Using an Aschoff Type I protocol (constant darkness) combined with 15-minute light pulses at circadian times (CT) 10, 14, and 22, we found that the absence of *Per1* in neurons—but not in astrocytes—significantly affected both the circadian period and phase advance shifts in response to light at CT22.

Keywords: light; resetting; phase shift; entrainment; advance; delay; *Per1* knockout

1. Introduction

The circadian system comprises organ- and tissue-specific clocks that regulate and synchronize physiological functions on a 24-hour time scale, aligning them with the environmental day-night cycle. Disruption of this alignment—such as that caused by shift work or jet lag—impairs the regulation of bodily functions and may ultimately contribute to metabolic syndrome, addictive behaviors, cardiovascular disease, and neurological disorders [1].

At the cellular level, the circadian clock operates through a transcriptional-translational feedback loop with an approximately 24-hour period. In mammals, the core clock genes include *Bmal1* and *Clock* (or its homolog *Npas2*), which activate the transcription of *Per* and *Cry* genes. These, in turn, inhibit their own activation, forming a negative feedback loop. The nuclear receptors REV-ERBα and RORα further regulate the expression of *Bmal1*, *Clock*, and *Npas2* by repressing or activating their transcription, respectively, thereby completing the core clock mechanism [2]. This mechanism can be modulated by: (1) molecules that bind to nuclear receptors—such as free fatty acids and glucocorticoids acting on PPARα and REV-ERBα—and (2) indirectly via glutamate and its receptors [3].

Circadian behavioral activity is primarily modulated by light. Changes in light intensity trigger adaptive responses, either advancing or delaying the organism's activity phase depending on the timing of exposure. For instance, a 15-minute light pulse late in the subjective night (e.g., circadian time 22; CT22) advances the clock phase, whereas light exposure early in the subjective night (e.g., CT14) delays it [4–6]. At the cellular level, light stimulates the release of neurotransmitters—such as glutamate—at synapses connected to the suprachiasmatic nuclei (SCN), the master pacemaker of the

 doi:10.20944/preprints202510.1246.v1

circadian system. This leads to the induction of immediate early genes, such as *Fos,* and clock genes, such as *Per1 and Per2* [7–9] [10,11].

Notably, mutation of the *Per2* gene in all cells of mice shortens the circadian period, diminishes phase delays, and enhances phase advances. In contrast, global deletion of *Per1* shortens the period and reduces phase advances only [12,13]. Cell-type-specific deletion of *Per2* in astrocytes or neurons also shortens the clock period, but only neuronal deletion affects phase shifts [14]. The distinct role of *Per1* in astrocytes and neurons regarding period regulation and phase-shifting remains unclear. Therefore, we investigated the contributions of *Per1* in these cell types to circadian period and light-induced phase-shifting responses.

2. Results

2.1. Per1 is Absent in Neuronal or Glial Knock-Out Mice

To investigate the cell type–specific role of *Per1* in regulating circadian period and light responsiveness, we generated glia-specific (*Per1*G; *Per1*/*Gfap-Cre*) and neuron-specific (*Per1*N; *Per1*/*Nes-Cre*) *Per1* knockout (KO) mice. Mice carrying a floxed *Per1* allele [15] (EMMA: 14846) were crossed with transgenic mice expressing *Cre*-recombinase under the control of either the *gfap*-promoter (*Gfap-Cre*, JAX: 004600) or the *nestin*-promoter (*Nes-Cre*, EMMA: EM04561).

To confirm cell type–specific deletion of *Per1* in neurons and astrocytes, we performed immunohistochemistry on suprachiasmatic nucleus (SCN) tissue harvested at ZT12 using PER1-specific antibodies (Fig. 1, green). Neurons were labeled with an anti-NeuN antibody (red) (Fig. 1A). In neuronal control mice (NCo; *Nes-Cre*), PER1 and NeuN co-localized, producing a yellow signal (Fig. 1A, upper row, white square at 5 μm). A 3D reconstruction of the neuron at 5 μm confirmed co-expression of PER1, NeuN, and the nuclear stain DAPI (blue), resulting in a yellow composite signal. In *Per1*NKo mice, PER1 expression was absent in neurons (Fig. 1A, lower row), indicating successful deletion of *Per1* in this cell type.

Astrocytes were labeled with an anti-GFAP antibody (Fig. 1B, magenta). In glial control mice (GCo; *Gfap-Cre*), PER1 and GFAP co-localized, producing a white signal (Fig. 1B, upper row, white square at 5 μm). A 3D reconstruction of the astrocyte at 5 μm showed co-expression of PER1, GFAP, and DAPI (blue), resulting in a white/cyan signal. In *Per1*GKo mice, PER1 expression was absent in astrocytes (Fig. 1B, lower row), confirming successful deletion of *Per1* in glial cells.

 doi:10.20944/preprints202510.1246.v1

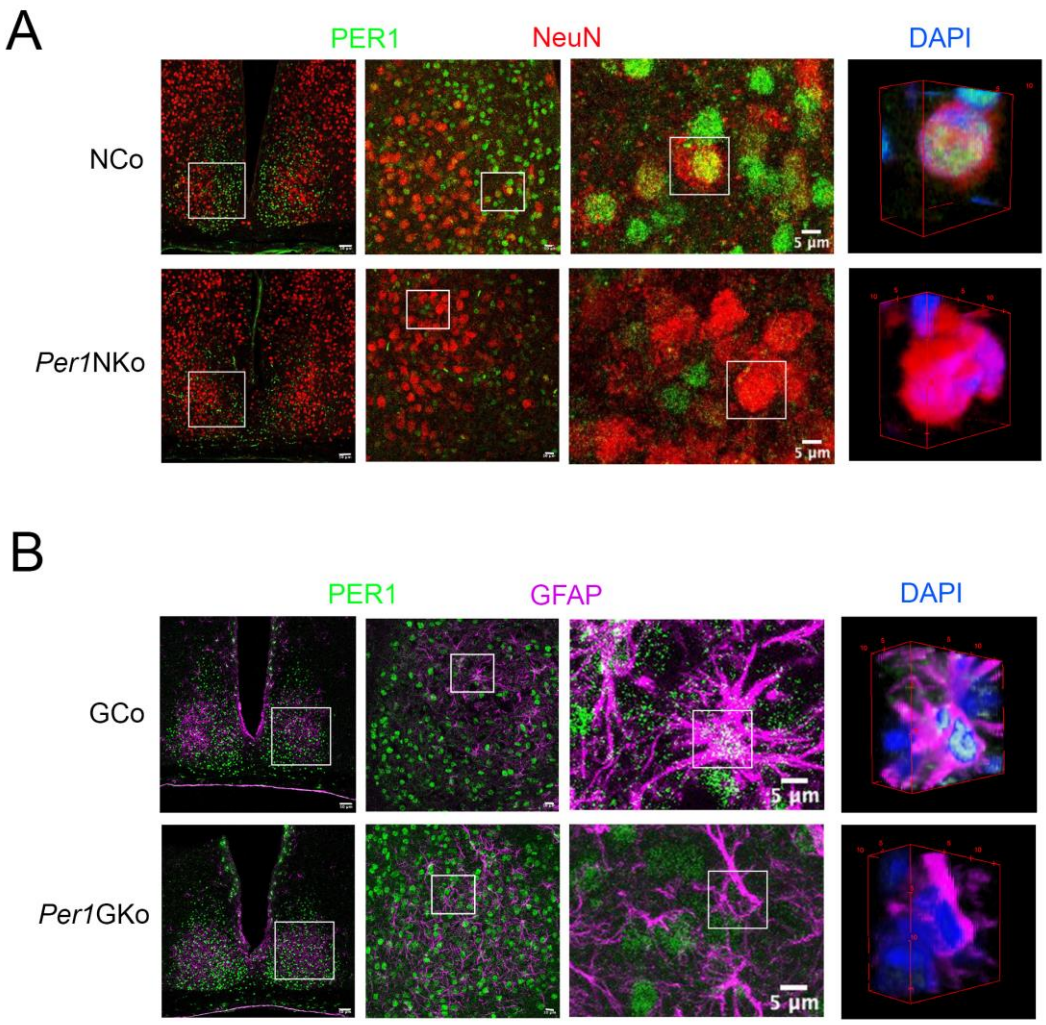

Figure 1. Immunohistochemistry of PER1 expression in the suprachiasmatic nuclei (SCN) of neuronal control (NCo), neuronal *Per1* knock-out (*Per1*NKo), glial control (GCo) and glial *Per1* knock-out (*Per1*GKo) mice at Zeitgeber time (ZT) 12. (**A**) Photomicrographs of SCNs from NCo and *Per1*NKO mice at low to high magnification (from left to right, white line = 50 µm, 10 µm, 5 µm). White squares indicate the magnified areas. The images at right show 3D reconstructions of cells with DAPI nuclear staining (blue). Green = PER1, red = NeuN specific to neuronal cells. (**B**) Photomicrographs of SCNs from GCo and *Per1*GKO mice at low to high magnification (from left to right, white line = 50 µm, 10 µm, 5 µm). White squares indicate the magnified areas. The images at right show 3D reconstructions of cells with DAPI nuclear staining (blue). Green = PER1, pink = glial fibrillary acidic protein (GFAP) specific to glial cells including astrocytes.

2.2. Lack of Per1 in Neuronal or Glial Knock-Out Mice Does not Abolish Circadian Rhythmicity but Slightly Reduces Phase Advances in Per1NKo Animals

To assess the impact of light on mice lacking *Per1* in neurons or astrocytes, we employed an Aschoff Type I protocol to evaluate light-induced rapid phase shifts under constant darkness [16,17]. The experimental design is illustrated in Figure 2 (see also Materials and Methods). All mouse strains were housed in constant darkness (DD) with access to a running wheel, and locomotor activity was recorded and visualized as double-plotted actograms (Fig. 3A).

 doi:10.20944/preprints202510.1246.v1

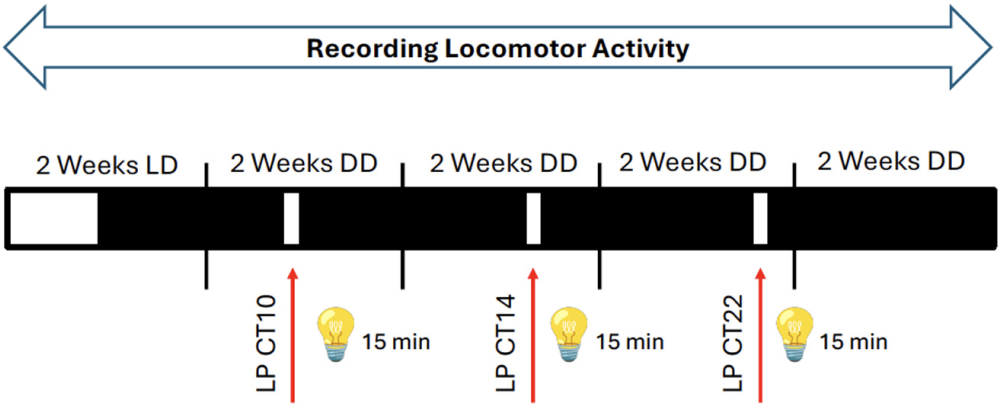

Figure 2. Experimental design for application of 15-minute light pulses (LPs, red arrows) using the Aschoff type I protocol. Mice were kept in a light / dark cycle (LD) for 2 weeks and then they were released into constant darkness (DD) before receiving a LP at circadian time (CT) 10. Subsequently, the animals were kept for 2 weeks in DD before they received a LP at CT14 (early subjective night). The mice were again kept for 2 weeks in DD and then they received a LP at CT22 (late subjective night). Subsequently, the animals were kept again in DD for 2 weeks. During the whole experiment locomotor activity was recorded. White and black bars represent light or dark, respectively.

After approximately 10 days in DD, animals received a 15-minute light pulse (LP) at circadian time (CT) 10, CT14, and CT22 (Fig. 3A, yellow stars). Following the LP, mice remained in DD, and activity onsets were marked with lines—blue for pre-LP and red for post-LP. The shift between blue and red lines was used to quantify phase delays or advances in activity onset.

Quantitative analysis revealed no significant effect of the LP at CT10 across all strains (Fig. 3B, left panel). The LP at CT14 induced phase delays that were consistent among all groups (Fig. 3B, middle panel). However, the LP at CT22 resulted in phase advances in all strains, with the exception of *Per1*NKo mice, which exhibited significantly reduced phase advances compared to controls and *Per1*GKo mice (Fig. 3B, right panel).

These findings suggest that *Per1* expression in neurons—but not in astrocytes—is involved in mediating light-induced phase advances in circadian behavior.

 doi:10.20944/preprints202510.1246.v1

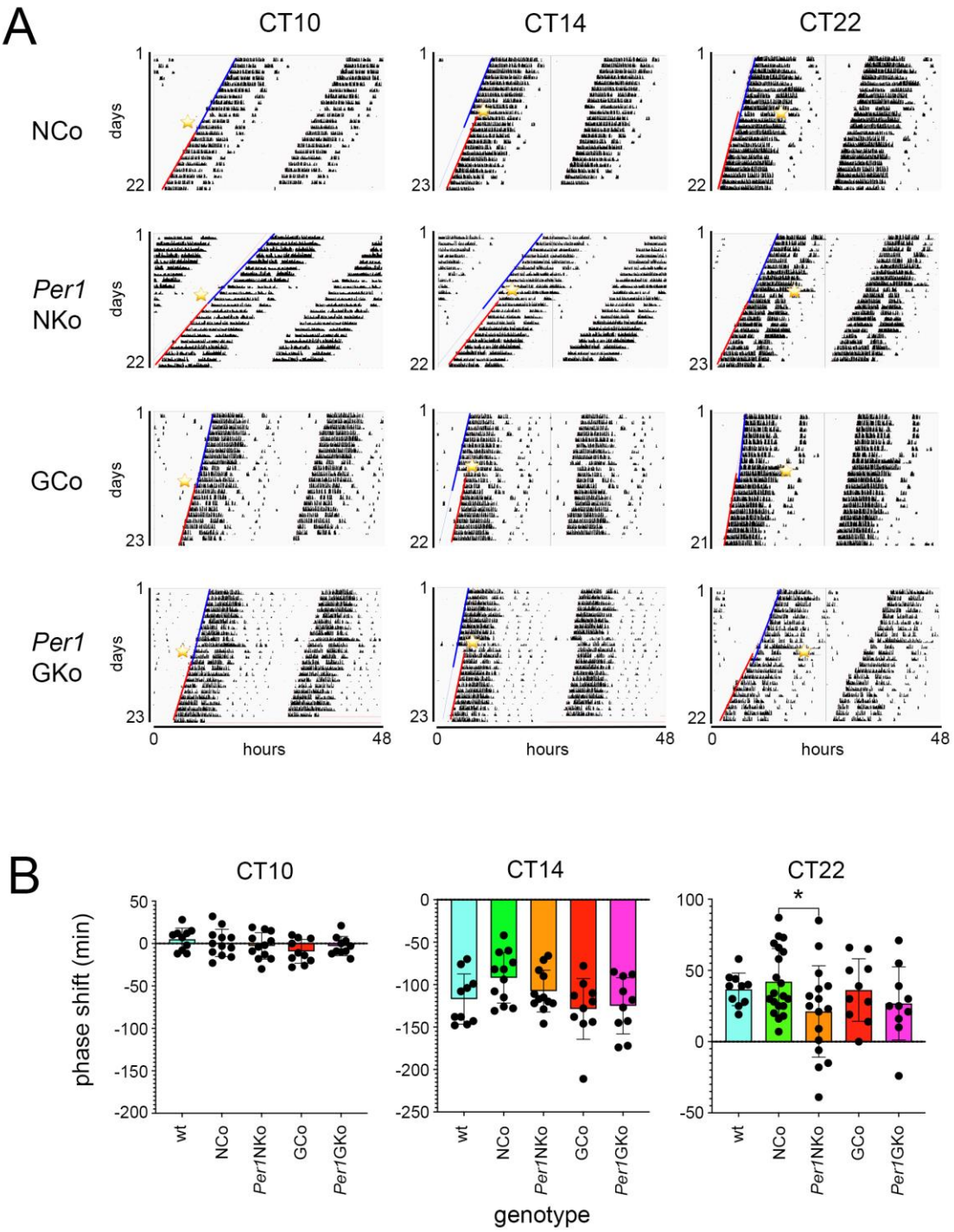

Figure 3. Wheel-running activity and effect of light pulses on control and cell type specific *Per1* knock-out mice under constant darkness (DD) conditions (Aschoff type I protocol). (**A**) Representative actograms of wheel-running activity of neuronal control (NCo), neuronal *Per1* knock-out (*Per1*NKo), glial control (GCo) and glial *Per1* knock-out (*Per1*GKo) animals. A 15-minute light pulse (LP) was applied at circadian time (CT) 10, 14, and 22 (yellow asterisk). The blue lines indicate onset of wheel-running activity before the LP and the red lines onset of activity after the LP. (**B**) Quantification of the distances between the blue and red lines in A representing the amount of phase shift in minutes after an LP at CT10 (left panel), CT14 (middle panel) and CT22 (right panel). Data are represented as mean ± SEM with n = 10 for wt (light blue), GCo (red), *Per1*GKo (pink) and n = 20 for NCo (green) and n = 16 for *Per1*NKo (orange). A diminished phase advance in *Per1* NKo mice was observed in response to an LP at CT22 (*$p < 0.05$, unpaired t-test).

 doi:10.20944/preprints202510.1246.v1

2.3. Period is Shortened In Mice Lacking Per1 in Neurons, And Light at CT22 Shortens Period Across All Strains

Using actograms derived from wheel-running activity recordings, we assessed the circadian period across all mouse strains. Notably, only mice lacking *Per1* in neurons (*Per1*NKo) exhibited a significantly shorter circadian period compared to their neuronal controls (NCo) under baseline conditions without LP (Fig. 4, § symbols). This finding aligns with previous reports of reduced phase advances in global *Per1* knockout mice [12,13].

We next examined whether light pulses at different circadian times affected the period. An LP at CT10 had no significant impact on period across all genotypes (Fig. 4A). Similarly, an LP at CT14 did not alter period in most strains, with the exception of *Per1*GKo mice, which showed a significant period shortening (Fig. 4B, purple and pink columns, * symbol).

Interestingly, an LP at CT22 resulted in a significant shortening of the circadian period in all genotypes examined (Fig. 4C, * symbols). This suggests that a light-sensitive signaling pathway is activated at CT22 and remains functional regardless of *Per1* deletion in either neurons or astrocytes.

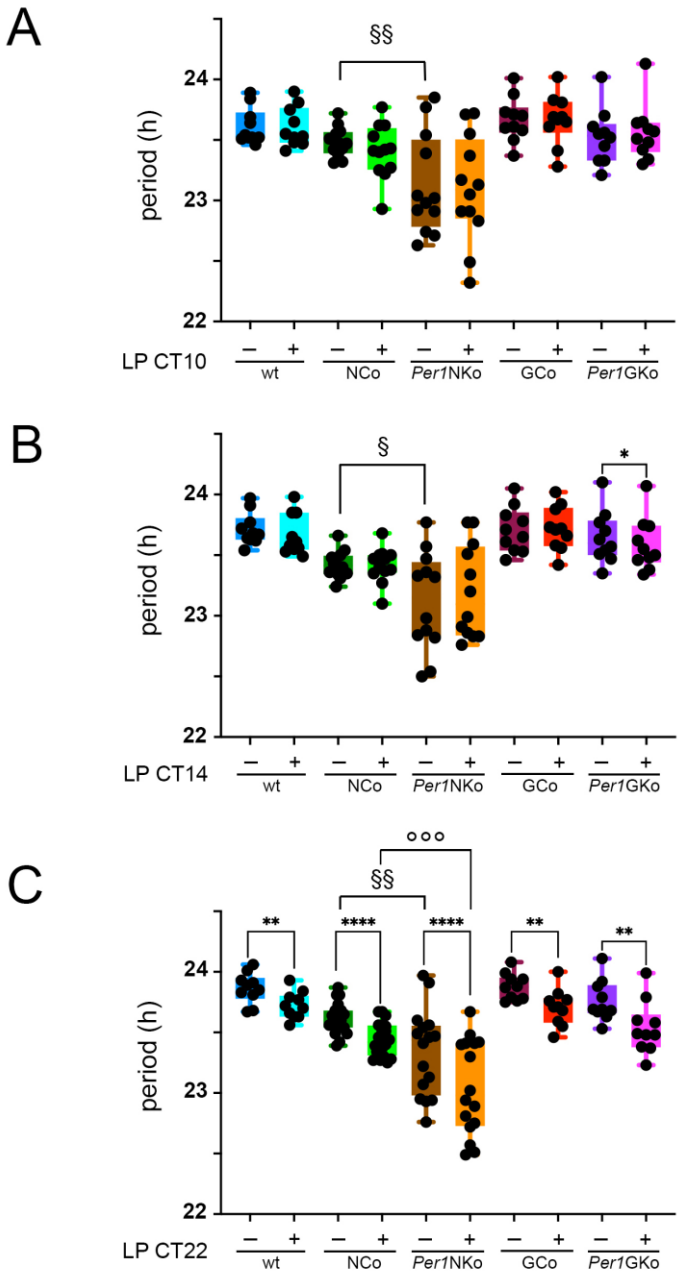

Figure 4. Period length in control (wt, NCo, GCo) and *Per1* knock-out animals (*Per1*NKo, *Per1*GKo) and effect of a light pulse (LP) on period. (**A**) Period before and after an LP at CT10 are similar in all genotypes investigated.

 doi:10.20944/preprints202510.1246.v1

Data are represented as mean ± SEM with n = 10-12. Period in *Per1*NKo mice (brown) before the LP is significantly shorter compared to NCo animals (dark green)(§§p < 0.01, n = 12, unpaired t-test). (**B**) Period before and after an LP at CT14 are similar in all genotypes investigated, except for *Per1*GKo mice which show a significantly shortened period after the LP (*p < 0.05, n = 10, Wilcoxon matched-pairs test). Data are represented as mean ± SEM with n = 10-12. Period in *Per1*NKo mice (brown) before the LP is significantly shorter compared to NCo animals (dark green)(§p < 0.05, n = 12, unpaired t-test). (**C**) Period before and after an LP at CT22 are significantly different in all genotypes investigated (**p < 0.01, n = 10 for wt, GCo, *Per1*GKo; ****p < 0.0001, n = 20 for NCo and 16 for *Per1*NKo, Wilcoxon matched-pairs test). Data are represented as mean ± SEM. Period in *Per1*NKo mice (brown) before the LP is significantly shorter compared to NCo animals (dark green)(§§p < 0.01, n = 16-20, unpaired t-test). Also after an LP at CT22 period in *Per1*NKo mice (orange) is significantly shorter compared to NCo animals (green)(°°°p < 0.001, n = 16-20, unpaired t-test).

2.4. Amplitude is Unaffected by Light Pulses but Reduced in Per1NKo Mice

We assessed circadian amplitude across all genotypes and found that light pulses (LPs) administered at CT10, CT14, and CT22 did not significantly alter amplitude in any group (Fig. 5A–C). However, *Per1*NKo mice exhibited a markedly reduced amplitude compared to their neuronal controls (Fig. 5A–C, middle panels, brown and orange columns), suggesting a potential weakening of the circadian oscillator in the absence of neuronal *Per1*.

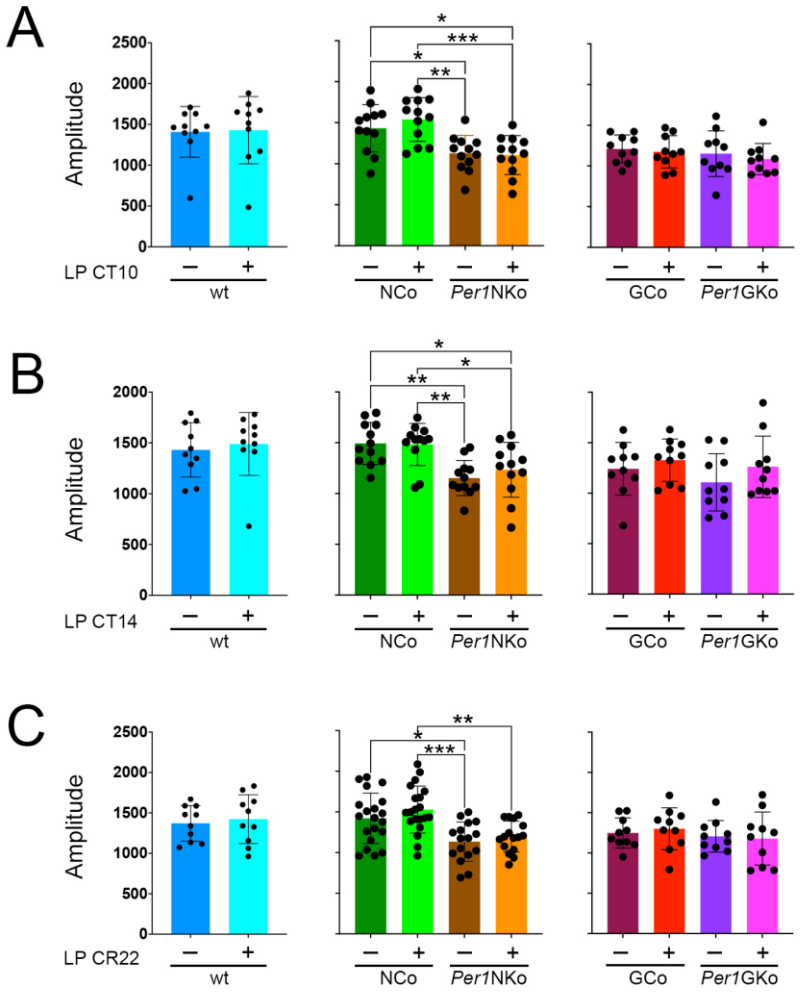

Figure 5. Amplitude in control (wt, NCo, GCo) and *Per1* knock-out animals (*Per1*NKo, *Per1*GKo) and effect of a light pulse (LP) on amplitude. (**A**) Amplitude before and after an LP at CT10 is similar in all genotypes investigated. Data are represented as mean ± SEM with n = 10-12. Amplitude in *Per1*NKo mice before (brown) and after (orange) the LP is significantly lower compared to NCo animals (green)(*p < 0.05, **p < 0.01, ***p < 0.001, n = 12, one-way ANOVA). (**B**) Amplitude before and after an LP at CT14 is similar in all genotypes

 doi:10.20944/preprints202510.1246.v1

investigated. Data are represented as mean ± SEM with n = 10-12. Amplitude in *Per1*NKo mice before (brown) and after (orange) the LP is significantly lower compared to NCo animals (green)(*p < 0.05, **p < 0.01, n = 12, one-way ANOVA). (**C**) Amplitude before and after an LP at CT22 is similar in all genotypes investigated. Data are represented as mean ± SEM with n = 10-12. Amplitude in *Per1*NKo mice before (brown) and after (orange) the LP is significantly lower compared to NCo animals (green)(**p < 0.01, ***p < 0.001, n = 12, one-way ANOVA).

To further investigate oscillator strength, we quantified the relative power of phase across genotypes (Fig. 6). Consistent with the observed shorter period and reduced amplitude, *Per1*NKo mice showed significantly lower relative power of phase compared to controls. No such reduction was observed in other strains. Additionally, light pulses did not affect relative power of phase in any genotype, corroborating findings from Figures 4 and 5.

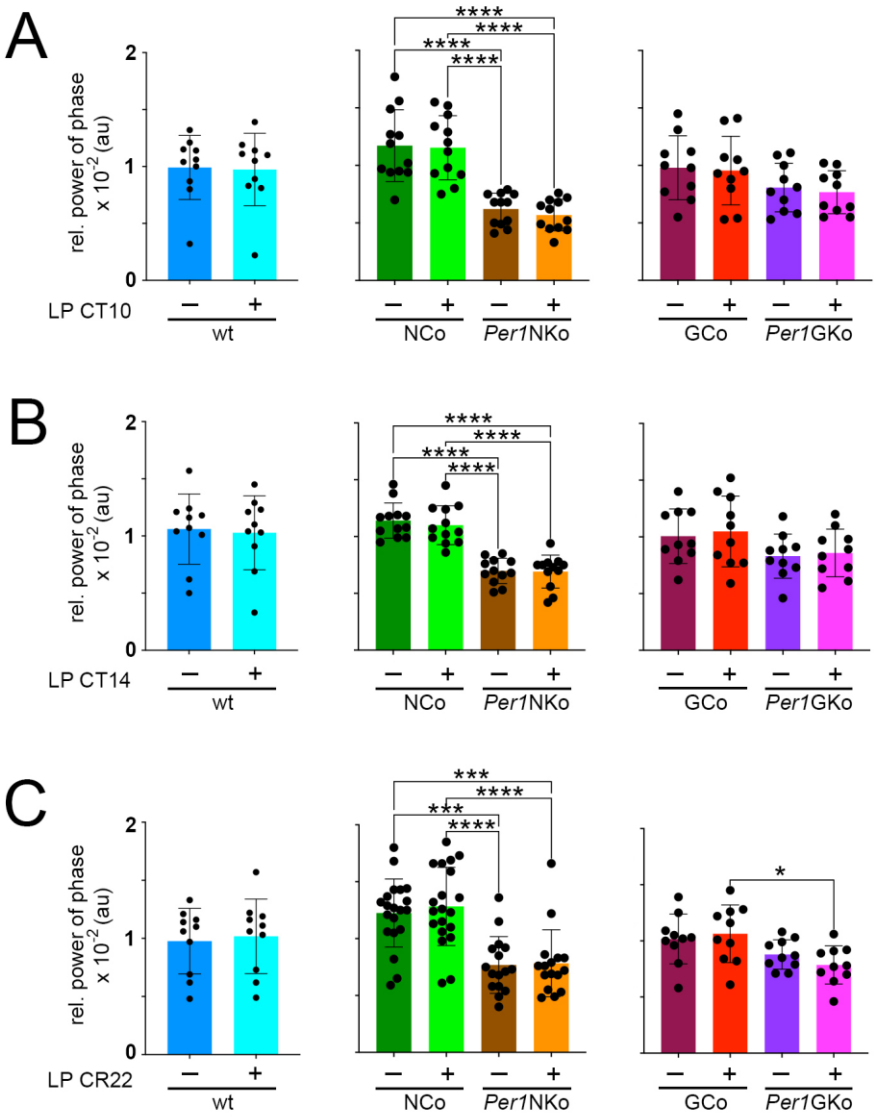

Figure 6. Relative power of phase in control (wt, NCo, GCo) and *Per1* knock-out animals (*Per1*NKo, *Per1*GKo) and effect of a light pulse (LP) on relative power of phase. (**A**) Relative power of phase before and after an LP at CT10 is similar in all genotypes investigated. Data are represented as mean ± SEM with n = 10-12. Relative power of phase in *Per1*NKo mice before (brown) and after (orange) the LP is significantly lower compared to NCo animals (green)(****p < 0.0001, n = 12, one-way ANOVA). (**B**) Relative power of phase before and after an LP at CT14 is similar in all genotypes investigated. Data are represented as mean ± SEM with n = 10-12. Relative power of phase in *Per1*NKo mice before (brown) and after (orange) the LP is significantly lower compared to NCo animals (green)(****p < 0.0001, n = 12, one-way ANOVA). (**C**) Relative power of phase before and after an LP at CT22 is similar in all genotypes investigated. Data are represented as mean ± SEM with n = 10-12. Relative

 doi:10.20944/preprints202510.1246.v1

power of phase in *Per1*NKo mice before (brown) and after (orange) the LP is significantly lower compared to NCo animals (green)(***p < 0.001, ****p < 0.0001, n = 12, one-way ANOVA). Relative power of phase in *Per1*GKo (magenta) is lower compared to GCo animals (red) after an LP at CT22 (*p < 0.05, n = 10, one-way ANOVA).

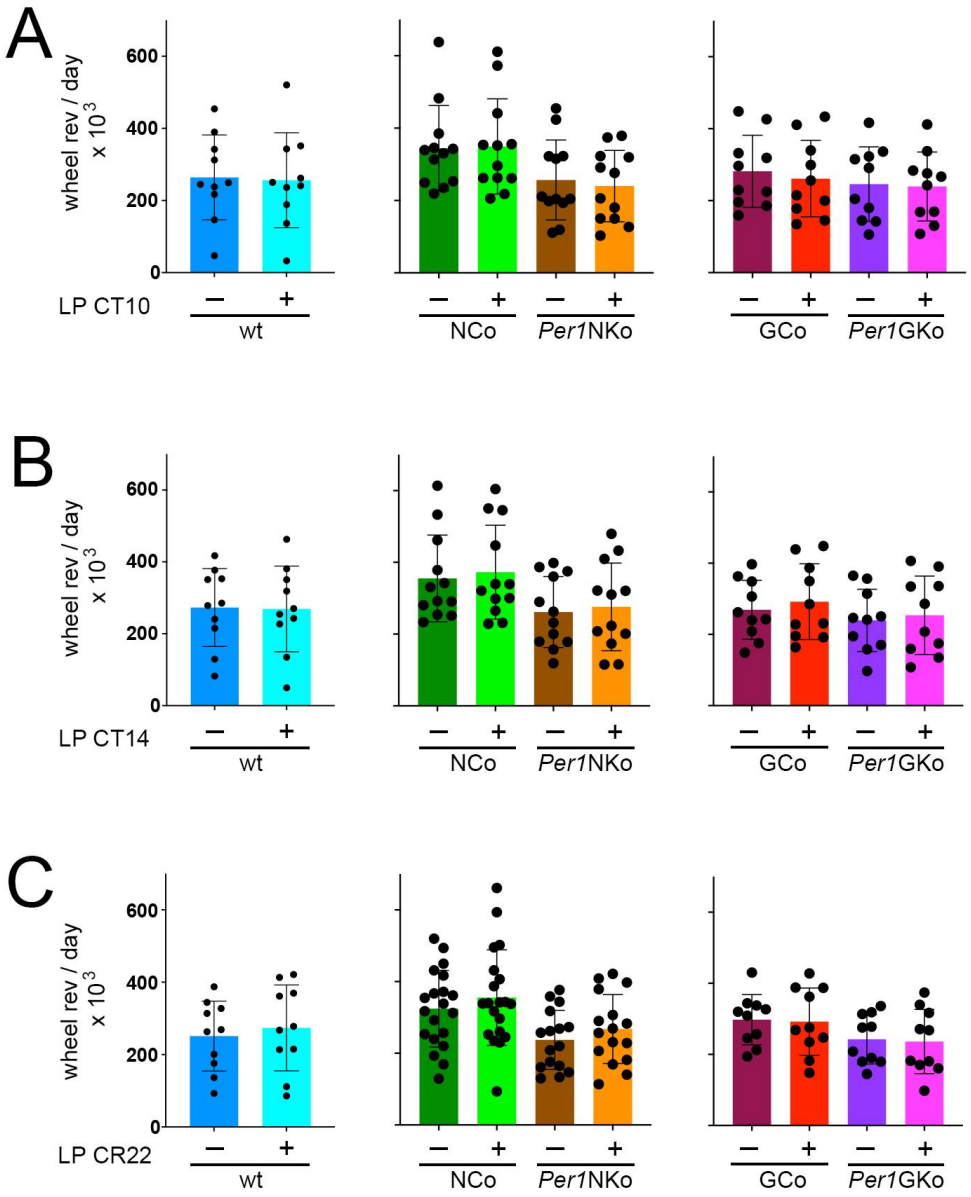

Figure 7. Total wheel-running activity in control (wt, NCo, GCo) and *Per1* knock-out animals (*Per1*NKo, *Per1*GKo) and effect of a light pulse (LP) on wheel-running activity. (**A**) Wheel revolutions per day before and after an LP at CT10 are similar in all genotypes investigated. Data are represented as mean ± SEM with n = 10-12. (**B**) Wheel revolutions per day before and after an LP at CT14 are similar in all genotypes investigated. Data are represented as mean ± SEM with n = 10-12. (**C**) Wheel revolutions per day before and after an LP at CT22 are similar in all genotypes investigated. Data are represented as mean ± SEM with n = 10-12.

Importantly, the differences between *Per1*NKo mice and controls were not attributable to changes in overall activity levels. Total wheel revolutions per day were comparable across all genotypes (Fig. 7A–C), indicating that the observed effects were specific to circadian parameters rather than general locomotor activity.

3. Discussion

 doi:10.20944/preprints202510.1246.v1

In this study, we investigated how the absence of the Per1 gene in neurons and astrocytes affects circadian period and phase, using wheel-running activity as a behavioral paradigm. Our experiments revealed that deletion of Per1 in astrocytes had no measurable impact on these parameters. In contrast, the absence of Per1 in neurons led to a shortened circadian period and diminished phase advances in response to a light pulse administered at CT22.

Previous studies have reported that *Per1::luc* reporter expression is undetectable in glial cells within organotypic SCN slice cultures from rat brain [18]. However, *Per1::luc* rhythms were observed in cultured astrocytes derived from cortical rat tissue [19]. This discrepancy suggests that *Per1* expression in astrocytes may be substantially lower or more diffuse than in neurons, where *Per1::luc* expression is readily detectable [18]. Our immunohistochemistry data support this interpretation (Fig. 1): we observed high levels of PER1 protein in SCN neurons (Fig. 1A), while PER1 signal in astrocytes was markedly lower (Fig. 1B).

Consistent with these findings, all behavioral circadian parameters assessed in mice lacking *Per1* in glial cells (*Per1*GKo) were indistinguishable from controls. Phase shifting remained unaffected (Fig. 3), period was comparable (Fig. 4), amplitude was normal (Fig. 5), and relative power of phase was unchanged (Fig. 6). Total wheel-running activity also matched that of control animals (Fig. 7). These results suggest that astrocytic *Per1* plays a minimal, if any, role in regulating behavioral circadian clock parameters *in vivo*.

In contrast, deletion of *Per1* in neurons resulted in reduced light-induced phase advances (Fig. 3), shortened period (Fig. 4), and decreased amplitude (Fig. 5), culminating in reduced relative power of phase (Fig. 6)—indicative of a weakened circadian oscillator. Notably, these changes were not attributable to differences in total wheel-running activity, which remained consistent across all groups. These findings, in line with previous reports [18], reinforce the notion that *Per1* primarily influences behavioral circadian parameters through neuronal mechanisms rather than astrocytic ones.

Several studies have demonstrated that *Per1* expression in the SCN can be induced by brief light exposure [7,10,11]. Moreover, global deletion of *Per1* in mice has been shown to impair phase advances without affecting phase delays [12], suggesting that light-induced *Per1* expression is specifically linked to phase advances. Our findings support and extend this view by showing that *Per1* expression in neurons—but not astrocytes—is necessary for light-induced phase advances (Fig. 3).

The reduction in phase advances observed in *Per1*NKo mice cannot be solely attributed to light-induced period shortening at CT22 (Fig. 4C). All genotypes exhibited period shortening following a light pulse at CT22, which could be interpreted as an earlier onset of activity the next day, contributing to the phase advances seen in Fig. 3. This effect was also present in *Per1*NKo mice (Fig. 4C, orange bar), and the difference in period between NCo and *Per1*NKo mice increased post-light pulse, with *Per1*NKo mice showing an even shorter period (Fig. 4C, §§ and °°°). If period shortening alone accounted for phase advances, *Per1*NKo mice would be expected to show greater advances than controls. However, the opposite was observed, indicating that *Per1*'s role in phase advancement in response to light at CT22 involves a molecular pathway distinct from its role in period regulation.

The functions of *Per1* and *Per2* genes appear to be distinct [12,20,21], and this distinction is evident when comparing their roles in neurons and astrocytes. In this study, we found that *Per1* in neurons—but not astrocytes—was critical for regulating period and phase advances. In contrast, *Per2* influenced period in both cell types, but only neuronal *Per2* was essential for phase delays [14]. This functional segregation aligns with previous reports showing that *Per1*-reporter expression is predominantly neuronal, while *Per2*-reporter expression is more restricted to non-neuronal populations [22]. Our findings also corroborate a recent study indicating that astrocytes regulate circadian period but not phase in the SCN [23].

In summary, astrocytic *Per1* appears to have limited importance for circadian regulation, whereas astrocytic *Per2* contributes to period control but not to light-mediated phase shifts. In neurons, both *Per* paralogs are essential: *Per1* for phase advances and *Per2* for phase delays.

 doi:10.20944/preprints202510.1246.v1

4. Materials and Methods

4.1. Housing of Mice and Mouse Strains

Male and female mice aged 2-6 months on a C57Bl/6 background were placed in isolated light cabinets as previously described in Jud et al., 2005 [24]. Entrainment was done in a constant 12:12 h light /dark cycle. Temperature (22 ± 2 °C monitored by temperature sensor, Technoline WS-9410, Berlin, Germany), humidity (40–50% monitored by humidity sensor, Technoline WS-9410, Berlin, Germany), and illumination (1000 Lux monitored by Luxmeter, Testo, GmbH & Co, Titisee-Neustadt, Germany) were kept constant in all cabinets. Each mouse was housed individually in cages (L: 280 mm × W: 105 mm × H: 125 mm) containing a running wheel made of steel (115 mm in diameter, Trixie GmbH, Tarp, Germany). All mice were provided with sufficient woodchip bedding, as to not block the running wheel, and enrichement materials such as: red-square house, piece of carton, neslet (5x5 cm) and an open-sided tube. Food and water were provided ad libitum.

The neuronal-specific *Per1*NKo (*Per1* fl/fl x *Nestin-cre*) and glia-specific *Per1*GKo (*Per1 fl/fl* x *Gfap-cre*) were obtained, by breeding the *Per1 fl/fl* mice described in Olejniczak et al., 2021; EMMA: 14846 [15] against the *Nestin-cre* mice [25](EMMA: EM04561) and *Gfap-cre* mice [26](JAX: 004600). The latter two mice lines were used as controls, along with the wild-type (WT) littermates. Glial and neuronal *Per1* deletion was verified by genotyping, and immunohistochemistry of brain tissues collected at zeitgeiber time (ZT) 12 (Fig. 1A-B). All experiments and procedures were performed according to the Schweizer Tierschutzgesetz guidelines and approved by the Canton of Fribourg and the cantonal commission for animal experiments (2021-17-FR, 33789).

4.2. Monitoring of Circadian Locomotor Activity Rhythm

To quantify the circadian locomotor activity rhythm, the running wheel revolutions were recorded by a magnetic circuit, which was fixed vertically on the axis of the running wheel outside the cage. The revolutions (locomotor activity) were captured in 1 minute intervals by ClockLab 3 data acquisition system software (Acquisition Version 3.208, Analysis Version 6.0.36). This is further described in Jud et al., 2005 [24]and Brenna et al., 2025 [27].

4.3. Light Pulses Application (Aschoff Type I Protocol)

The experimental designed (Fig. 2) was designed and performed according to the Aschoff Type I protocol [16,17]. Mice were allowed to entrain in a constant 12:12 light:dark cycle for 2 weeks. This was followed by their release into constant darkness (DD) for 2 weeks, switching off the light by using an automatic digital timer. Following the 2 weeks in DD, the light pulse (LP) at circadian time (CT) 10 was calculated for each mouse individually by analysing their wheel running activity in the ClockLab3 software. In essence, the last 10 days of wheel running activity in DD were used to obtain the period length, and prediction of activity at CT12 for the next day. These were used to calculate the light pulse at CT10 for each mouse, as described in Jud et al., 2005 [24]. The LPs were applied the next day in a separate cabinet. Each mouse received a 15 minute LP at their previously calculated time, followed by their transfer into the original cabinet, where they were allowed to run freely for another 2 weeks in DD. The procedure described above, was repeated for administering the LPs at CT14 and CT22 (Fig. 2). At the end of the last DD entrainement, the mice were transferred back into a 12:12 light:dark cycle. A recovery time of 2 weeks was allowed, before they were sacrificed for tissue collection.

4.4. Analysis of Circadian Locomotor Activity Rhythm Parameters

Phase shift (i.e., phase resetting) in DD following each LP, as well as other circadian locomotor activity rhythm parameters (e.g., actograms, period length, amplitude, total locomotor activity count, and relative power of phase (FFT)) were evaluated using ClockLab analysis (Actimetrics) software version 6.0.36.

 doi:10.20944/preprints202510.1246.v1

To calculate the phase shift following each light pulse, a line of best fit was set through 10 consecutive activity onsets before the LP was applied. A second line of best fit was set through 10 activity onsets after the LP, excluding the first two days after the LP (transition phase). The difference between the two lines of best fit at the onset of activity, during the day of the LP, is considered the phase shift value.

All other circadian locomotor activity parameters were obtained using the ClockLab3 softaware, by setting the 2 lines of best fit through 10 activty onsets as described above.

4.5. Tissue Collections and Immunohistochemistry

Mice were perfused at ZT12 with 4% paraformaldehyde (PFA). Brains were isolated, with particular care in not damaging the optical nerve area and subsequently the SCN. Brains were held overnight in 4% PFA before being cryoprotected in 30% sucrose for 2 days. SCN cryosections (40 μm) from each brain, were placed in 24-well plates. Sections were washed for 20 min. in 1x PBS buffer, followed by 3 times 10-min washes in 1x PBS/0.2% Triton X-100 buffer. The sections were then treated for 15 min. in 1x PBS/1% Triton X-100m buffer, before being washed again 3 times with 1x PBS/0.2% Triton X-100. Sections were then blocked for 3 h at room temperature in 1x PBS/ 0.2% Triton X-100/ 10% Donkey Serum (Sigma, Catalog Number D9663). Following blocking, primary antibodies for PER1, GFAP, NeuN (Table 1), were diluted in 1x PBS/ 0.2% Triton X-100/ 10% Donkey Serum and sections were incubated at 4° C for 2 nights. Following incubation, the sections were washed 5 times (10 min. each) with 1x PBS/0.2% Triton X-100 buffer, before being incubated for 2 h at room temperature with the secondary antibodies (Table 1), diluted in 1x PBS/ 0.2% Triton X-100/ 10% Donkey Serum. This was then followed by 5 times washes with 1x PBS/ 0.2% Triton X-100, and an overnight wash at 4° C. All sections were stained with DAPI (Roche; 1:5000 in 1x PBS/ 0.2% Triton X-100) for 20 minutes. A final wash with 1x PBS/ 0.2% Triton X-100 was performed before being mounted on glass microscope slides. Fluorescent Z-stacks images were taken using a confocal microscope (Leica TCS SP5) using either the 20x or 63x magnification. All acquired images were processed in ImageJ, version 2.14.0/ 2.54f. The images of the SCN for each mouse genotype, acquired with either the 20x or 63x magnification, were analyzed by compressing the entire Z-stack. On the other hand, for the 3D analysis, no compression of the Z-stack was performed.

Table 1. Antibodies used for immunohistochemistry.

Antibody	Species	Company	Catalog number	Lot Number	Dilution
Anti-mPER1 (residues 6-21)	Rabbit	Merck Millipore	AB2201	3480987	1:8000
Anti-GFAP	Goat	Abcam	AB53554	1046529-1	1:1000
Anti-NeuN	Chicken	Merck Millipore	ABN91	4049831	1:2000
Alexa Fluor 647- AffiniPure Donkey Anti-Chicken IgG (H+L)	Donkey	Jackson Immunoresearch	703-605-155	134612	1:1000
Alexa Fluor 568 Donkey Anti-Goat IgG (H+L)	Donkey	Abcam	Ab175704	GR3278446-1	1:1000

 doi:10.20944/preprints202510.1246.v1

Alexa Fluor 488-AffiniPure Donkey Anti-Rabbit IgG (H+L)	Donkey	Jackson Immunoresearch	711-545-152	132876	1:1000

4.6. Statistical Analysis

GraphPad Prism software (version 10.3.1) was used for statistical analysis. Parametric unpaired t-test was used to calculate the significant difference between the groups, in the phase shift following each light pulse. A similar test was used to quantify the differences in the period lengths between the cell-specific KOs and their controls. On the other hand, a parametric paired t-test was used to calculate the significant difference in the period lengths before and after LPs for each group. In addition, the significant difference between three groups or more was performed using parametric one-way ANOVA, using the Tukey test to correct for multiple comparisons. Data are presented as mean ± SEM, and are considered significant when the p value < 0.05.

The raw data appear in Appendix A.

Author Contributions: Conceptualization, D.E. and U.A.; methodology, D.E.; validation, D.E, and U.A.; formal analysis, D.E.; investigation, D.E.; resources, U.A.; data curation, D.E.; writing—original draft preparation, U.A.; writing—review and editing, D.E.; visualization, U.A.; supervision, U.A.; project administration, U.A.; funding acquisition, U.A. All authors have read and agreed to the published version of the manuscript.

Funding: This research was funded by the Swiss National Science Foundation, grant number 310030_219880/1 (U.A.) and the State of Fribourg.

Institutional Review Board Statement: All experiments and procedures were performed according to the Schweizer Tierschutzgesetz guidelines and approved by the Canton of Fribourg and the cantonal commission for animal experiments (2021-17-FR, 33789).

Informed Consent Statement: Not applicable

Data Availability Statement: The original contributions presented in this study are included in the article. Further inquiries can be directed to the corresponding author.

Acknowledgments: The authors thank Antoinette Hayoz, Maude Marmy and Dr. Jürgen Ripperger for technical support and Dean Stewart and Spyridoula Mitsikosta for critically reading the manuscript.

Conflicts of Interest: The authors declare no conflicts of interest.

Appendix A

Raw Data

Figure 3B

Phase Shift- LP CT10				
WT	**NCo**	***Per1*NKO**	**GCo**	***Per1*GKo**
12	7	-4	0	0
-2	-23	-18	-26	21
-12	-16	19	-28	-10
-12	23	17	-14	-9
28	32	-2	7	7
10	0	-30	-17	-9
7	10	6	6	-18

 doi:10.20944/preprints202510.1246.v1

15	-3	15	10	-12
12	7	-18	-11	-3
-8	-14	-13	-20	3
	-10	3		
	-5	-9		

Phase Shift- LP CT14

WT	NCo	*Per1*NKO	GCo	*Per1*GKo
-147	-108	-115	-138	-127
-138	-115	-129	-120	-85
-70	-74	-120	-110	-172
-99	-60	-66	-113	-90
-108	-42	-71	-144	-108
-76	-82	-117	-128	-143
-143	-62	-90	-78	-174
-104	-128	-122	-99	-145
-138	-94	-111	-146	-118
-148	-82	-122	-211	-88
	-131	-83		
	-126	-146		

Phase Shift- LP CT22

WT	NCo	*Per1*NKO	GCo	*Per1*GKo
39	7	39	50	25
30	34	25	65	39
40	28	-18	28	30
44	30	-6	39	55
58	25	9	30	21
19	32	-39	19	25
45	18	30	0	-24
39	16	1	51	71
28	74	21	14	10
25	20	32	66	16
	87	37		
	41	23		
	69	-15		
	66	48		
	73	67		
	58	85		
	25			
	45			
	30			
	63			

 doi:10.20944/preprints202510.1246.v1

 doi:10.20944/preprints202510.1246.v1

Fig4 A– Period Length- With and Without LP CT10

WT -	WT +	NCo -	NCo +	P1NKO -	P1NKO +	GCo -	GCo +	P1GKO -	P1GKO +
23.52	23.52	23.72	23.77	22.63	22.49	23.7	23.67	23.7	23.64
23.52	23.47	23.32	23.25	22.71	22.91	24.01	24.02	23.33	23.51
23.69	23.9	23.43	23.41	23.04	23.13	23.88	23.81	23.52	23.48
23.46	23.48	23.42	22.93	23.85	23.72	23.61	23.69	23.61	23.57
23.54	23.65	23.47	23.4	23.54	23.55	23.73	23.83	23.55	23.59
23.51	23.41	23.31	23.27	23.39	23.37	23.6	23.65	23.21	23.3
23.52	23.53	23.63	23.62	23.02	23.05	23.37	23.28	23.56	23.65
23.89	23.81	23.48	23.53	22.91	22.32	23.5	23.69	23.33	23.34
23.84	23.75	23.38	23.42	22.74	22.83	23.71	23.41	23.45	23.42
23.64	23.55	23.55	23.22	22.92	22.91	23.58	23.61	24.02	24.13
		23.57	23.62	22.98	23.17				
		23.51	23.43	23.77	23.71				

Fig4 B- Period Length- With and Without LP CT14

WT -	WT +	NCo -	NCo +	P1NKo -	P1NKo +	GCo -	GCo +	P1GKo -	P1GKo +
23.54	23.53	23.4	23.4	22.98	22.99	23.71	23.73	23.77	23.75
23.64	23.58	23.36	23.35	22.84	22.76	24.05	24.02	23.57	23.38
23.91	23.85	23.66	23.5	23.32	23.2	23.83	23.88	23.47	23.46
23.67	23.49	23.31	23.37	23.57	23.77	23.78	23.72	23.63	23.62
23.62	23.56	23.5	23.5	23.33	23.51	23.61	23.58	23.54	23.48
23.68	23.61	23.24	23.27	23.36	23.34	23.92	23.92	23.35	23.34
23.72	23.55	23.54	23.1	22.5	22.83	23.46	23.42	23.83	23.55
23.97	23.98	23.47	23.51	22.88	22.91	23.54	23.56	23.7	23.74
23.77	23.85	23.48	23.47	23.47	23.59	23.65	23.71	23.51	23.5
23.63	23.65	23.43	23.68	22.54	22.83	23.53	23.66	24.1	24.07
		23.34	23.38	22.82	22.86				
		23.35	23.47	23.77	23.77				

Fig4 C- Period Length- With and Without LP CT22

WT -	WT +	NCo -	NCo +	P1NKO -	P1NKO +	GCo -	GCo +	P1GKO -	P1GKO +
23.85	23.56	23.59	23.51	22.94	22.51	23.78	23.71	23.92	23.79
23.81	23.79	23.54	23.56	23.56	22.94	24.08	24	23.69	23.58
24.01	23.84	23.67	23.67	23.13	22.75	23.94	23.82	23.53	23.37
23.91	23.63	23.49	23.39	23.46	23.41	23.87	23.77	23.79	23.6
23.67	23.63	23.68	23.28	23.6	23.4	23.76	23.68	23.67	23.48
23.68	23.72	23.81	23.67	23.97	23.48	23.99	23.76	23.63	23.23
23.89	23.7	23.6	23.27	23.49	23.3	23.79	23.59	23.69	23.48
24.06	23.93	23.56	23.5	23.47	23.41	23.88	23.46	23.68	23.38
23.93	23.77	23.39	23.27	23.22	23.02	23.94	23.55	23.88	23.49

 doi:10.20944/preprints202510.1246.v1

23.83	23.66	23.65	23.46	22.93	22.57	23.75	23.71	24.11	23.99
		23.87	23.25	22.76	22.72				
		23.81	23.64	22.95	22.49				
		23.54	23.4	23.54	23.42				
		23.49	23.44	23.41	22.89				
		23.56	23.37	23.07	22.81				
		23.58	23.3	23.91	23.67				
		23.73	23.56						
		23.42	23.39						
		23.64	23.34						
		23.68	23.55						

Fig 5A- Amplitude- With and Without LP CT10

WT -	WT +		
1629.2	1673.6		
596.2	484.83		
1630.28	1651.32		
1291.7	1170.19		
1708.38	1881.72		
1462.28	1744.38		
1477	1625.51		
1394.99	1103.68		
1476.33	1515.13		
1412.77	1442.94		
NCo -	**NCo +**	**P1NKO -**	**P1NKO +**
1566.23	1630.78	1022.9	914.22
1367.67	1368.14	679.31	631.27
1525.49	1519.59	1533.5	1309.38
1895.58	1911.1	1269.11	1179.53
1394.79	1565.67	1256.69	1470.32
1588	1784.54	911.89	784.27
1150.29	1185.78	1092.38	1123.25
879.61	1120.03	1180.42	1047.43
1737.62	1769.17	1187.93	1174.27
1405.35	1654.24	1305.9	1262.47
1066.06	1186.45	961.34	1060.84
1604.57	1771.29	1110.39	1303.44
GCo -	**GCo +**	**P1GKO -**	**P1GKO +**
1420.29	1181	968.53	1097.58
1253.68	1146.13	1232.85	920.71
1043.8	887.32	1291.7	1170.19
934.56	910.72	963.98	893.04

 doi:10.20944/preprints202510.1246.v1

1346.69	1362.21	1464.79	1534.84
1029.59	1106.36	1274.09	1088.74
1421.2	1427.64	1051.08	970.53
1320.21	1469.69	1006.68	907.49
1172.18	1173.28	1609.85	1195.26
1147.91	1064.07	639.8	1062.97

Fig 5B- Amplitude- With and Without LP CT14

WT -	WT +		
1700.28	1731		
1025.83	679.8		
1793.12	1658.44		
1561.66	1578.08		
1716.78	1780.54		
1443.52	1616.54		
1046.23	1413.56		
1347.69	1433.07		
1385.71	1511.1		
1288.71	1491.23		
NCo -	**NCo +**	**P1NKO -**	**P1NKO +**
1675.76	1615.08	1234.96	1048.78
1494.18	1429.02	831.3	664.68
1676.09	1520.32	1414.74	1535.74
1322.45	1534.78	1452.98	1378.7
1438.15	1531.97	1205.68	1464.62
1769.83	1535.75	1083.32	1289.99
1408.81	1089.65	1057.86	1185.5
1281.54	1504.97	1066.39	1207.54
1320.81	1573.63	1015.99	1270.6
1580.79	1650.43	1246.28	1575.57
1794.14	1747.38	1156.43	1331.06
1154.33	1057.54	1063.21	855.05
GCO -	**GCo +**	**P1GKO -**	**P1GKO +**
1420.29	1181	968.53	1097.58
1253.68	1146.13	1232.85	920.71
1043.8	887.32	1291.7	1170.19
934.56	910.72	963.98	893.04
1346.69	1362.21	1464.79	1534.84
1029.59	1106.36	1274.09	1088.74
1421.2	1427.64	1051.08	970.53
1320.21	1469.69	1006.68	907.49
1172.18	1173.28	1609.85	1195.26

 doi:10.20944/preprints202510.1246.v1

1147.91	1064.07	639.8	1062.97

Fig 5C- Amplitude- With and Without LP CT22

WT -	WT +		
1073.47	1062.06		
1670.84	1784.74		
1476.21	1601.83		
1588.3	1832.59		
1135.89	1156.47		
1479.6	1327.47		
1116.26	961.53		
1339.08	1521.42		
1587.32	1640.92		
1238.91	1340.14		
NCo -	**NCO +**	**P1NKO -**	**P1NKO +**
1481.56	1529.37	1227.28	1189.36
1624.38	1409.12	1023	850.79
1861.74	1676.92	1244.99	1461.47
1448.02	1667.55	1381.32	1438.58
1255.35	1497.07	727.42	1241.72
1375.49	1412.21	1274.48	1178.82
959.37	1068.34	691.59	936.2
1819.02	1752.56	971.88	1207.46
997.71	961.52	1174.01	1162.88
1150.3	1556.34	1051.52	1034.11
1033.47	1434.64	1496.9	1440.03
1427.15	1426.25	894.46	984.58
1296.44	1384.99	1364.76	1330.06
961.63	1306.92	1176.71	1194.95
1586.6	2086.73	989.71	1076.45
1902.79	1823.62	1450.16	1423.16
1261.72	1206.29		
1539.68	1891.81		
1927.48	1987.97		
1508.26	1490.64		
GCo -	**GCo +**	**P1GKO -**	**P1GKO +**
1518.92	1282.65	1070.15	785.52
1405.78	1383.96	1371.63	1299.42
1252.48	1127.76	1319.08	1325.03
1522.85	1714.34	1139.27	1006.39
952.73	1042.12	1631.8	1721.83
1175.99	1458.97	966.08	1253.66

 doi:10.20944/preprints202510.1246.v1

1280.26	1409.2	1021.15	818.92
1136.51	1507.97	1235.66	1200.19
1133.49	794.41	1098.63	1591.71
1102.36	1276.25	1208.2	780.88

Fig 6A- Relative Power of Phase- With and Without LP CT10

WT -	WT +		
0.0115	0.0119		
0.0032	0.0022		
0.0104	0.0105		
0.01	0.0089		
0.0121	0.0139		
0.0114	0.0114		
0.008	0.0081		
0.0132	0.011		
0.0087	0.0083		
0.0106	0.0111		
NCo -	**NCo +**	**P1NKO -**	**P1NKO +**
0.0102	0.0098	0.0049	0.0049
0.0095	0.0093	0.0041	0.0033
0.0094	0.0075	0.0076	0.0068
0.0149	0.0155	0.0052	0.0044
0.0097	0.0092	0.0079	0.0076
0.0127	0.0129	0.0044	0.0045
0.0156	0.0144	0.0075	0.007
0.007	0.008	0.0075	0.0072
0.0094	0.0112	0.0068	0.0062
0.0119	0.012	0.0068	0.0052
0.0126	0.0134	0.005	0.0046
0.0177	0.0152	0.0068	0.0065
GCo -	**GCo +**	**P1GKO -**	**P1GKO +**
0.0098	0.0093	0.0053	0.0055
0.0082	0.008	0.0077	0.0065
0.007	0.0053	0.007	0.0061
0.01	0.0095	0.0058	0.0055
0.0055	0.0054	0.0088	0.0083
0.0077	0.0088	0.01	0.0092
0.0145	0.0141	0.0111	0.0102
0.011	0.0107	0.0081	0.0064
0.0131	0.0139	0.0109	0.0101
0.0112	0.0105	0.006	0.0089

 doi:10.20944/preprints202510.1246.v1

Fig 6B- Relative Power of Phase- With and Without LP CT14

WT -	WT +
0.0121	0.0123
0.005	0.0033
0.0116	0.0103
0.0104	0.0104
0.0118	0.0121
0.0124	0.0129
0.0062	0.0069
0.0157	0.0145
0.0101	0.0091
0.0107	0.011

NCo -	NCo +	P1NKO -	P1NKO +
0.0108	0.0107	0.0053	0.0046
0.0095	0.0095	0.0051	0.0042
0.0099	0.0094	0.007	0.0075
0.0107	0.0102	0.0078	0.0094
0.0138	0.0127	0.0068	0.0056
0.0105	0.0112	0.0084	0.0078
0.0118	0.0086	0.0085	0.0073
0.0099	0.0104	0.0076	0.0069
0.0119	0.0145	0.0079	0.0075
0.0118	0.0124	0.0067	0.0075
0.0146	0.0125	0.006	0.007
0.0117	0.0099	0.0066	0.0077

GCo -	GCo +	P1GKO -	P1GKO +
0.0093	0.0095	0.0046	0.0055
0.0094	0.0084	0.0073	0.0072
0.0086	0.0077	0.0077	0.0073
0.0122	0.011	0.0068	0.0061
0.0062	0.0059	0.0088	0.0097
0.0119	0.0135	0.0091	0.0098
0.014	0.0152	0.0089	0.011
0.0089	0.0077	0.0079	0.0083
0.0122	0.0119	0.0101	0.0089
0.0079	0.014	0.0118	0.012

 doi:10.20944/preprints202510.1246.v1

Fig 6C- Relative Power of Phase- With and Without LP CT22

WT -	WT +		
0.0048	0.0049		
0.0114	0.0116		
0.0097	0.0103		
0.011	0.0119		
0.0069	0.0073		
0.0121	0.0122		
0.0133	0.0157		
0.0116	0.0111		
0.0062	0.0062		
0.0106	0.0106		
NCo -	**NCo +**	**P1NKO -**	**P1NKO +**
0.0106	0.0113	0.0058	0.0055
0.0129	0.0106	0.0054	0.0049
0.0118	0.0101	0.0091	0.0069
0.0121	0.0123	0.0095	0.0083
0.0082	0.0115	0.0058	0.0068
0.0065	0.0061	0.0073	0.0083
0.0125	0.0166	0.004	0.0048
0.0168	0.0173	0.0115	0.0122
0.0125	0.0136	0.0075	0.0086
0.0133	0.011	0.0071	0.0079
0.0059	0.0064	0.0069	0.0068
0.0143	0.0124	0.0085	0.0076
0.0105	0.0098	0.0049	0.0053
0.0132	0.0166	0.0068	0.0072
0.0108	0.0126	0.0092	0.0076
0.0143	0.0132	0.0136	0.0166
0.0144	0.0159		
0.0127	0.0138		
0.0137	0.0185		
0.018	0.0169		
GCo -	**GCo +**	**P1GKO -**	**P1GKO +**
0.0103	0.0098	0.0071	0.0046
0.01	0.0101	0.0079	0.007
0.008	0.0082	0.0085	0.0078
0.0102	0.0128	0.0071	0.0064
0.0058	0.0061	0.0108	0.0089
0.0105	0.0116	0.0087	0.0091
0.0096	0.0122	0.0103	0.0092
0.0139	0.0145	0.0096	0.0077

 doi:10.20944/preprints202510.1246.v1

0.0109	0.0126	0.008	0.0106
0.0125	0.0084	0.0099	0.0072

Fig 7A- Wheel Revolutions- With and Without LP CT10

WT -	WT +		
244734	240866		
46792	32568		
237729	236200		
217243	188537		
454149	520440		
249152	250230		
146302	136451		
389652	342849		
312362	262004		
341940	351375		
NCo -	**NCo +**	**P1NKO -**	**P1NKO +**
218791	205467	111072	126750
252929	217789	119075	102913
342744	262696	322705	276080
482338	572646	204308	149835
313478	355716	193381	180136
330132	295652	198051	206006
637773	610999	203996	150433
234887	261367	454497	374048
384940	441118	423743	378609
339336	353439	315264	322637
345426	352075	210797	291156
249229	261962	322166	319490
GCo -	**GCo +**	**P1GKO -**	**P1GKO +**
296336	255942	105882	107544
229251	214979	144644	130187
185580	134745	179670	168521
195696	178052	204501	169353
159084	144890	290940	275816
224838	199862	416302	411713
448138	433318	336436	337461
318614	339488	314908	242631
426093	410714	322923	266675
331914	299191	142074	283565

 doi:10.20944/preprints202510.1246.v1

Fig 7B- Wheel Revolutions- With and Without LP CT14

WT -	WT +		
240410	254367		
82311	49743		
285137	242927		
215179	227147		
376859	462758		
278298	270004		
129260	134719		
417326	380632		
352962	318603		
350868	350632		
NCo -	**NCo +**	**P1NKO -**	**P1NKO +**
251290	231417	156910	115182
280599	265181	118707	115494
342037	339369	262451	321276
254022	320806	289847	310230
533059	446784	178316	207862
292090	300417	231630	200888
378389	550061	386629	432737
233259	228652	178930	173431
613617	604298	200160	222907
461801	545264	398227	479472
290516	298258	374886	409356
330929	339254	360278	320689
GCo -	**GCo +**	**P1GKO -**	**P1GKO +**
262020	285084	96965	107620
306433	230807	157855	134910
175325	191835	170113	174704
242560	195258	194854	207609
148531	163719	241263	285885
362979	386668	356582	406299
397118	448138	314382	335690
239686	227843	246404	334522
348745	349613	364804	390672
208570	438812	250504	159382

Fig 7C- Wheel Revolutions- With and Without LP CT22

WT -	WT +
92557	85671
262836	277889
200624	213688
313694	421147

 doi:10.20944/preprints202510.1246.v1

175633	214912		
268751	267469		
136337	111548		
387280	413122		
344158	369719		
327321	361340		
NCo -	**NCo +**	**P1NKO -**	**P1NKO +**
239390	234918	160751	140374
312436	260558	129961	113624
354334	342854	219735	256441
317156	337413	257202	282733
169070	244920	133229	168874
128860	93636	146894	230736
416713	502006	176013	181463
519500	593352	272844	290042
292209	296689	165029	228320
371353	386950	376412	397206
193241	229756	268641	378746
431143	431138	358247	421444
361284	406581	208696	206332
256446	338402	317752	306705
252999	339745	343732	408438
338345	341841	261867	268968
366863	317026		
219944	252265		
493689	660953		
449941	495378		
GCo -	**GCo +**	**P1GKO -**	**P1GKO +**
256610	234705	145045	97931
308817	275293	179235	160647
246088	182287	179498	170569
212203	247235	190443	182077
194307	148037	313510	268019
337609	387877	277649	374044
326693	427769	318375	316719
343640	387117	275483	270982
430180	268466	207919	339585
319850	362163	335811	180523

References

1. Roenneberg, T.; Merrow, M. The Circadian Clock and Human Health. *Curr Biol* **2016**, *26*, R432-443, doi:10.1016/j.cub.2016.04.011.

2. Takahashi, J.S. Transcriptional architecture of the mammalian circadian clock. *Nat Rev Genet* **2017**, *18*, 164-179, doi:10.1038/nrg.2016.150.
3. Albrecht, U. Timing to perfection: the biology of central and peripheral circadian clocks. *Neuron* **2012**, *74*, 246-260, doi:10.1016/j.neuron.2012.04.006.
4. Daan, S.; Pittendrigh, C.S. A function analysis of circadian pacemakers in nocturnal rodents. II. The variability of phase response curves. *J. Comp. Physiol.* **1976**, *106*, 253-266.
5. Schwartz, W.J.; Zimmerman, P. Circadian timekeeping in BALB/c and C57BL/6 inbred mouse strains. *J Neurosci* **1990**, *10*, 3685-3694, doi:10.1523/JNEUROSCI.10-11-03685.1990.
6. Foster, R.G.; Hughes, S.; Peirson, S.N. Circadian Photoentrainment in Mice and Humans. *Biology (Basel)* **2020**, *9*, doi:10.3390/biology9070180.
7. Albrecht, U.; Sun, Z.S.; Eichele, G.; Lee, C.C. A Differential Response of Two Putative Mammalian Circadian Regulators, mper1and mper2, to Light. *Cell* **1997**, *91*, 1055-1064, doi:https://doi.org/10.1016/S0092-8674(00)80495-X.
8. Dziema, H.; Oatis, B.; Butcher, G.Q.; Yates, R.; Hoyt, K.R.; Obrietan, K. The ERK/MAP kinase pathway couples light to immediate-early gene expression in the suprachiasmatic nucleus. *Eur J Neurosci* **2003**, *17*, 1617-1627, doi:10.1046/j.1460-9568.2003.02592.x.
9. Golombek, D.A.; Rosenstein, R.E. Physiology of circadian entrainment. *Physiol Rev* **2010**, *90*, 1063-1102, doi:10.1152/physrev.00009.2009.
10. Shigeyoshi, Y.; Taguchi, K.; Yamamoto, S.; Takekida, S.; Yan, L.; Tei, H.; Moriya, T.; Shibata, S.; Loros, J.J.; Dunlap, J.C.; et al. Light-Induced Resetting of a Mammalian Circadian Clock Is Associated with Rapid Induction of the mPer1 Transcript. *Cell* **1997**, *91*, 1043-1053, doi:https://doi.org/10.1016/S0092-8674(00)80494-8.
11. Yan, L.; Silver, R. Differential induction and localization of mPer1 and mPer2 during advancing and delaying phase shifts. *Eur J Neurosci* **2002**, *16*, 1531-1540, doi:10.1046/j.1460-9568.2002.02224.x.
12. Albrecht, U.; Zheng, B.; Larkin, D.; Sun, Z.S.; Lee, C.C. MPer1 and mper2 are essential for normal resetting of the circadian clock. *J Biol Rhythms* **2001**, *16*, 100-104, doi:10.1177/074873001129001791.
13. Spoelstra, K.; Albrecht, U.; van der Horst, G.T.; Brauer, V.; Daan, S. Phase responses to light pulses in mice lacking functional per or cry genes. *J Biol Rhythms* **2004**, *19*, 518-529, doi:10.1177/0748730404268122.
14. Hassan, S.A.; Wendrich, K.S.; Albrecht, U. Deletion of Clock Gene Period 2 (Per2) in Astrocytes Shortens Clock Period but Does Not Affect Light-Mediated Phase Shifts in Mice. *Clocks Sleep* **2025**, *7*, doi:10.3390/clockssleep7030037.
15. Olejniczak, I.; Ripperger, J.A.; Sandrelli, F.; Schnell, A.; Mansencal-Strittmatter, L.; Wendrich, K.; Hui, K.Y.; Brenna, A.; Ben Fredj, N.; Albrecht, U. Light affects behavioral despair involving the clock gene Period 1. *PLoS Genet* **2021**, *17*, e1009625, doi:10.1371/journal.pgen.1009625.
16. Aschoff, J. Circadian Rhythms in Man. *Science* **1965**, *148*, 1427-1432, doi:10.1126/science.148.3676.1427.
17. Pittendrigh, C.S. Circadian Systems: Entrainment. In *Biological Rhythms*, Aschoff, J., Ed.; Springer: Boston, MA, USA, **1981**; pp. 95-124.
18. Yamaguchi, S.; Isejima, H.; Matsuo, T.; Okura, R.; Yagita, K.; Kobayashi, M.; Okamura, H. Synchronization of cellular clocks in the suprachiasmatic nucleus. . *Science* **2003**, *302*, 1408–1412.
19. Prolo, L.M.; Takahashi, J.S.; Herzog, E.D. Circadian rhythm generation and entrainment in astrocytes. *J Neurosci* **2005**, *25*, 404-408, doi:10.1523/JNEUROSCI.4133-04.2005.
20. Abarca, C.; Albrecht, U.; Spanagel, R. Cocaine sensitization and reward are under the influence of circadian genes and rhythm. *Proc Natl Acad Sci U S A* **2002**, *99*, 9026-9030, doi:10.1073/pnas.142039099.
21. Park, J.; Lee, K.; Kim, H.; Shin, H.; Lee, C. Endogenous circadian reporters reveal functional differences of PERIOD paralogs and the significance of PERIOD:CK1 stable interaction. *Proc Natl Acad Sci U S A* **2023**, *120*, e2212255120, doi:10.1073/pnas.2212255120.
22. Cheng, H.Y.; Alvarez-Saavedra, M.; Dziema, H.; Choi, Y.S.; Li, A.; Obrietan, K. Segregation of expression of mPeriod gene homologs in neurons and glia: possible divergent roles of mPeriod1 and mPeriod2 in the brain. *Hum Mol Genet* **2009**, *18*, 3110-3124, doi:10.1093/hmg/ddp252.

 doi:10.20944/preprints202510.1246.v1

23. Patton, A.P.; Smyllie, N.J.; Chesham, J.E.; Hastings, M.H. Astrocytes Sustain Circadian Oscillation and Bidirectionally Determine Circadian Period, But Do Not Regulate Circadian Phase in the Suprachiasmatic Nucleus. *J Neurosci* **2022**, *42*, 5522-5537, doi:10.1523/JNEUROSCI.2337-21.2022.
24. Jud, C.; Schmutz, I.; Hampp, G.; Oster, H.; Albrecht, U. A guideline for analyzing circadian wheel-running behavior in rodents under different lighting conditions. *Biol Proced Online* **2005**, *7*, 101-116, doi:10.1251/bpo109.
25. Tronche, F.; Kellendonk, C.; Kretz, O.; Gass, P.; Anlag, K.; Orban, P.C.; Bock, R.; Klein, R.; Schütz, G. Disruption of the glucocorticoid receptor gene in the nervous system results in reduced anxiety. *Nature Genetics* **1999**, *23*, 99-103, doi:10.1038/12703.
26. Zhuo, L.; Theis, M.; Alvarez-Maya, I.; Brenner, M.; Willecke, K.; Messing, A. hGFAP-cre transgenic mice for manipulation of glial and neuronal function in vivo. *Genesis* **2001**, *31*, 85-94, doi:10.1002/gene.10008.
27. Brenna, A.; Ripperger, J.A.; Albrecht, U. Locomotor Activity Monitoring in Mice to Study the Phase Shift of Circadian Rhythms Using ClockLab (Actimetrics). *Bio Protoc* **2025**, *15*, e5187, doi:10.21769/BioProtoc.5187.